Semiconductor Block Copolymer Nanocomposites with Lamellar Morphology via Self-Organization

Sébastien Maria,[†] Andrei S. Susha,[‡] Michael Sommer,[†] Dmitri V. Talapin,[§] Andrey L. Rogach,[‡] and Mukundan Thelakkat*,[†]

Applied Functional Polymers, Universität Bayreuth, Universitätsstr. 30, 95444 Bayreuth, Germany; Photonics and Optoelectronics Group, Physics Department and Center for Nanoscience (CeNS), Ludwig-Maximilians Universität München, Amalienstr. 54, 80799 Munich, Germany; and Department of Chemistry, The University of Chicago, Chicago, Illinois 60637

Received April 3, 2008; Revised Manuscript Received June 9, 2008

ABSTRACT: Novel semiconductor block copolymers were synthesized using nitroxide-mediated radical polymerization (NMRP). They are comprised of a hole conductor block carrying tetraphenylbenzidine pendant units (PVDMTPD) and a second poly(4-vinylpyridine) (P4VP) block suitable for the preferential incorporation of n-type semiconductor nanocrystals. The conditions of NMRP for both monomers were optimized in order to get macroinitiators with well-defined molecular weights and very low polydispersity (<1.2). The resulting block polymers exhibit a lamellar morphology due to microphase separation. Furthermore, semiconductor nanocomposites were prepared using these diblock copolymers and light harvesting CdSe:Te nanocrystals, and their bulk morphologies were characterized by TEM. This new hybrid nanocomposite material maintains the original lamellar structure in which the hole conductor domains are separated from electron conducting/light harvesting nanocrystals that are confined in the P4VP domains. Thus, the challenging task of applying the block copolymer strategy to obtain fully functionalized semiconductor hybrid nanocomposites with morphological control and stability has been realized.

Introduction

Polymer nanocomposites are one of the innovative approaches in material science to tune material properties suitable for novel applications.[1,2] A common strategy is to blend nanoobjects such as nanodots, nanorods, etc., in a polymer matrix to obtain the required mechanical, optical, electrical, or magnetic properties in thin films.[3,4] For example, solar cells with good efficiency were obtained from a hybrid blend of n-type semiconductor CdSe nanocrystals and p-type poly(3-hexylthiophene).[5]

The use of block copolymers instead of homopolymers as matrix material has been reported recently, which allows a better control of the spatial distribution of the nanoparticles. This is achieved by exploiting the order−disorder phase transition in block copolymers, which leads to well-defined morphologies at the nanometer scale.[6–11] One of the major issues in developing nanoparticle/polymer composites is how to stabilize the hybrid blend against macrophase separation or agglomeration of the nanoparticles. Such a phase separation negates any benefits associated with the unique nanoscopic dimensions of the particles. Usually the nanoparticles agglomerate over time, and therefore, they have to be surface-modified with electronically inactive tensides. It would be elegant if one segment of a block copolymer could serve as a multidental ligand for the nanocrystals while the other one takes care of the complementary electronic function. This would result in self-organizing nanocomposites with well-defined morphologies at the nanoscopic scale,[12–14] which could lead to novel concepts in the fields of spintronics[15] or photovoltaics. However, this concept is challenging and requires tailor-made semiconductor block copolymers carrying different functionalities for charge separation, charge transport, and additional segments which stabilize the nanoparticles. Previously, we reported microphase-separated donor−acceptor block copolymers[16–18] with poly(perylene bisimide acrylate) (PPerAcr) as electron conducting segment and several poly(vinyltriarylamine)s as hole conducting segments.[16] The morphologies of these block copolymers play a crucial role in improving the performance of solar cells compared to a blend of the respective homopolymers.[17,18]

In this paper, we report the synthesis and characterization of functional diblock copolymers, poly(vinyl-*N,N′*-bis(4-methoxyphenyl)-*N,N′*-diphenyl-(1,1′-biphenyl)-4,4′-diamine)-*block*-poly(4-vinylpyridine), PVDMTPD-*block*-P4VP. In such a system, P4VP can stabilize electron conducting/light harvesting nanoparticles against agglomeration, whereas the PVDMTPD acts as a hole transporting block. After incorporating inorganic semiconductor quantum dots, this hybrid system can lead to nanostructured bulk heterojunctions suitable for solar cell applications. In order to accomplish this task, we prepared a series of PVDMTPD-*block*-P4VP by nitroxide-mediated radical polymerization (NMRP). First, the polymerization conditions of 4-vinylpyridine were optimized in order to get P4VP macroinitiators with well-defined molecular weights and very low polydispersity (<1.2). The morphology of different block copolymers, PVDMTPD-*block*-P4VP, was studied in the bulk using transmission electron microscopy (TEM). Polymer nanocomposites using these block copolymers and light harvesting CdSe:Te nanocrystals were prepared, and the first results of self-organizing semiconductor hybrid nanostructures are presented.

Results and Discussion

NMRP of 4VP. Up to now, the controlled/living polymerization of 4VP has been carried out successfully by anionic polymerization.[19] If one uses atom transfer radical polymerization (ATRP), the polymerization reaction is quite tedious due to the possible coordination of the monomer 4VP with the catalyst.[20] In contrast, reversible addition−fragmentation chain transfer polymerization (RAFT)[21] and nitroxide-mediated radical polymerization (NMRP) do not require transition metal complexes and therefore are suitable for the polymerization of 4VP. Relatively a few reports deal with NMRP of 4VP using 2,2,6,6-

* Corresponding author. E-mail: Mukundan.Thelakkat@uni-bayreuth.de.
[†] Universität Bayreuth.
[‡] Ludwig-Maximilians Universität München.
[§] The University of Chicago.

10.1021/ma8007459 CCC: $40.75
Published on Web 07/30/2008

Scheme 1. (a) Scheme of Synthesis of P4VP Using NMRP; (b) Mechanism Showing the NMRP Equilibrium of Poly(4-vinylpyridine) Chain Growth

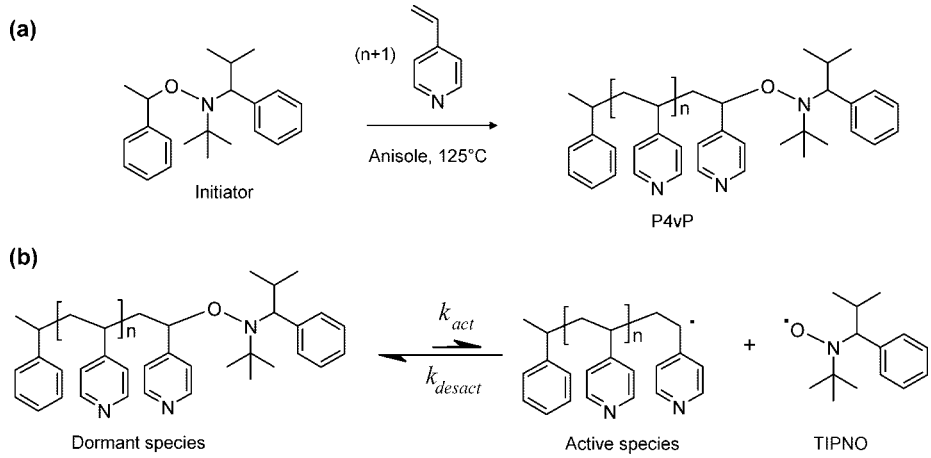

tetramethyl-1-piperidine-*N*-oxyl (TEMPO) as a free radical.[22–24] To our knowledge, only one report used an alkoxyamine generating the nitroxide 2,2,5-trimethyl-4-phenyl-3-azahexane-3-oxyl (TIPNO).[25]

First, we studied the polymerization of 4VP by NMRP in bulk and in solution. This is required to obtain macroinitiators with defined length and narrow polydispersity that are suitable for the synthesis of defined block copolymers using functional monomers such as vinyl-*N,N′*-bis(4-methoxyphenyl)-*N,N′*-diphenyl-(1,1′biphenyl)-4,4′-diamine (VDMTPD). The scheme of synthesis of P4VP and the mechanism of NMRP are shown in Scheme 1.

The bulk polymerization of 4VP was carried out at 125 °C with a $[monomer]_0$:$[initiator]_0$:$[TIPNO]_0$ molar ratio of 318:1:0.07. The initial addition of TIPNO allows shifting the equilibrium, as shown in Scheme 1b, to the side of the dormant species and reduces the instantaneous concentration of growing radicals due to the persistent radical effect. The polymerization proceeded relatively fast (42% conversion after 1 h), and the first-order monomer consumption rate was investigated by plotting $\ln([M]_0/[M])$ vs time (Figure 1a). The plot does not reveal a straight line, but is slightly curved, indicating that the concentration of active radicals is not constant throughout the polymerization as expected for a controlled process. Hence, the polymerization does not take place under steady-state conditions; e.g. termination occurs continuously, resulting in a decrease of the transient radical concentration and an increase of the free nitroxide concentration. Nevertheless, this does not significantly affect the control of the polymerization. The molecular weights were measured by size exclusion chromatography (SEC) and are in good agreement with the theoretical values calculated on the basis of the monomer-to-initiator ratio (see Figure 1b). Moreover, the polydispersity indices (PDI) are quite small (∼1.2). This might be a consequence of the fast rate of polymerization compared to the rate of bimolecular termination. Table 1 summarizes the data of samples under different conditions of polymerization; in each case two samples at two different conversions are given for each batch of polymerization. The data of the two samples that were drawn during bulk polymerization at two different conversions, **1a** and **1b**, are given in Table 1.

One way to limit the bimolecular termination and to improve the control of polymerization is to increase the initial ratio of $[TIPNO]_0$:$[initiator]_0$. Therefore, two additional polymerizations were conducted with $[4VP]_0$:$[initiator]_0$:$[TIPNO]_0$ molar ratios of 321:1:0.12 and 294:1:0.19. Thus, compared to the first bulk polymerization, the relative amount of initial free nitroxide was augmented from 1:0.07 to 1:0.12 and 1:0.19. Additionally, the polymerization mixture was slightly diluted with anisole to a [4VP]:[anisole] volume ratio of 5:1. Now, the plots of $\ln([M]_0/[M])$ vs time show a perfect linear behavior in both cases (see Figure 2). Consequently, the rate of the monomer consumption is first-order, and the concentration of the active radical can be considered constant throughout the polymerization.

Another interesting question is to check the equation of the linear regression of the plots. The difference of the values of the slope is quite small. For the two different polymerizations with $[4VP]_0$:$[initiator]_0$:$[TIPNO]_0$ equal to 321:1:0.12 and 294:1:0.19, the apparent rate constant of polymerization (k_{app}) is equal to 10.4×10^{-3} and 9.47×10^{-3} min^{-1}, respectively. Thus, for the polymerization with the highest concentration of TIPNO,

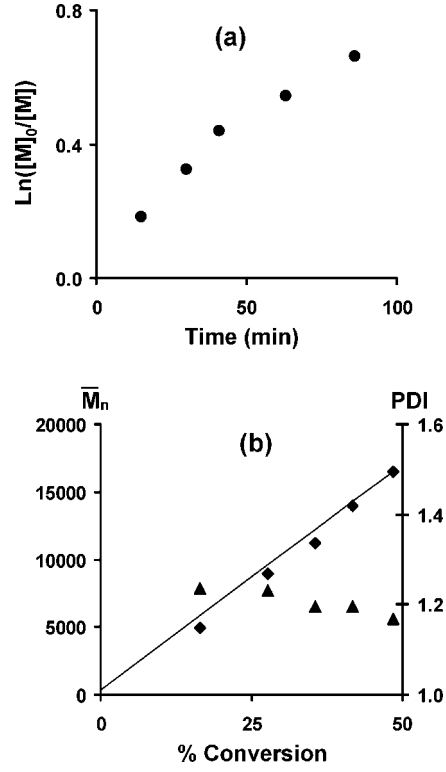

Figure 1. Kinetics and control of 4VP polymerization in bulk at 125 °C: (a) pseudo-first-order kinetics; (b) M_n (diamonds) and PDI (triangles) as a function of conversion. The straight line corresponds to the theoretical M_n values. [4VP]:[initiator]:[TIPNO] is equal to 318:1:0.07.

Table 1. Experimental Conditions, Molecular Weights, Polydispersity Indices, and Conversion of Macroinitiators 1a−g and 2a−d (M: Monomer; I: Initiator; Solvent: Anisole)

macroinitiator	number	$[M]_0$ (wt %)	conversion (%)	$[M]_0$:$[I]_0$:$[TIPNO]_0$ molar ratio	M_n (kg/mol)	M_w (kg/mol)	PDI
P4VP	**1a**	bulk	16.6	318:1:0.07	4.9	6.1	1.24
	1b	bulk	41.9	318:1:0.07	14.0	16.7	1.20
	1c	82.4	13.7	320:1:0.12	4.7	6.1	1.28
	1d	82.4	38.7	320:1:0.12	13.6	15.6	1.15
	1e	82.4	8.6	294:1:0.19	3.4	3.9	1.16
	1f	82.4	44.4	294:1:0.19	14.0	16.0	1.14
	1g	82.4		295:1:0.2	14.9	16.8	1.13
PVDMTPD	**2a**	43.7	47.5	74:1:0.9	10.6	12.1	1.14
	2b	43.7	77.3	74:1:0.9	12.5	15.5	1.24
	2c	78.1		200:1:0.2	13.3	16.3	1.23
	2d	24.9		120:1:0.1	20.8	23.9	1.15

k_{app}, is slightly smaller, as expected. The small difference can be attributed to growing radicals that are provided by autoinitiation, maintaining a reasonable rate of polymerization and

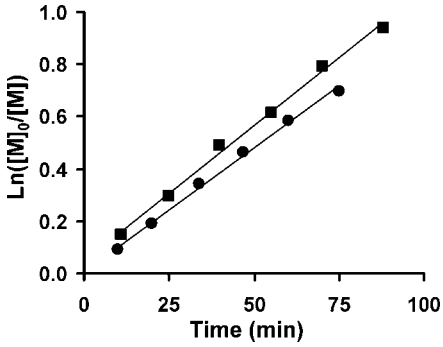

Figure 2. Influence of the concentration of free nitroxide on the first-order kinetics of the polymerization of P4VP in anisole (5:1, v:v) at 125 °C: [4VP]:[initiator]:[TIPNO] is equal to 321:1:0.12 (diamonds) and 294:1:0.19 (circles).

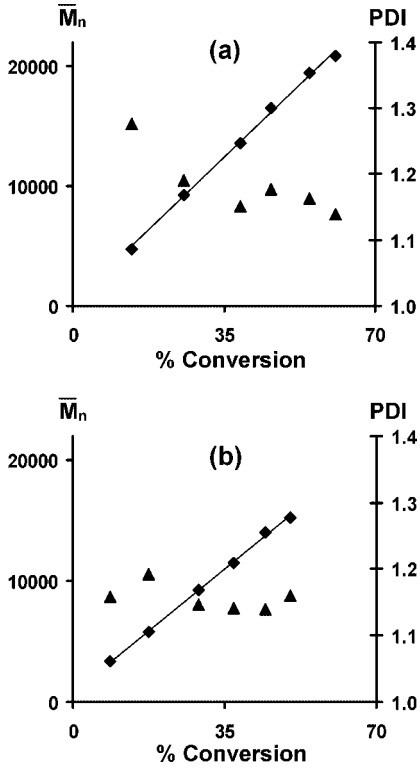

Figure 3. Influence of the free nitroxide concentration on the control of 4VP polymerization in anisole (5:1, v:v) at 125 °C: M_n (diamonds) and PDI (triangles) as a function of conversion. The molar ratios [4VP]:[initiator]:[TIPNO] are equal to 321:1:0.12 (a) and 294:1:0.19 (b). The straight line corresponds to the theoretical M_n values.

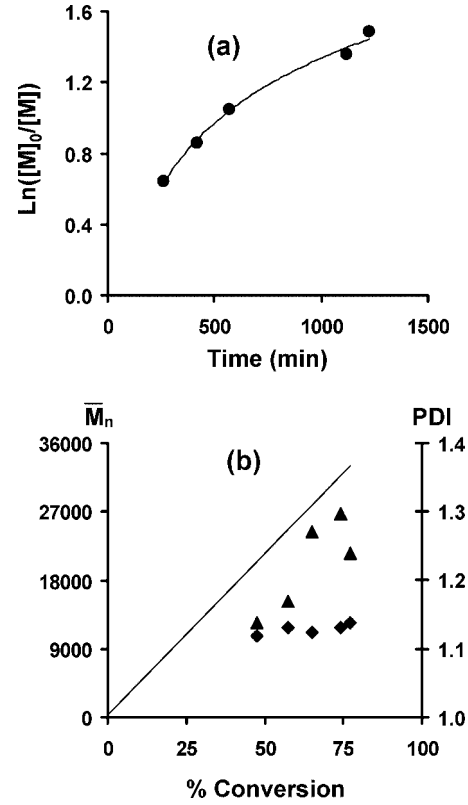

Figure 4. Polymerization of VDMTPD in anisole at 125 °C: (a) first-order kinetics; (b) M_n (diamonds) and PDI (triangles) as a function of conversion. The straight line corresponds to the theoretical M_n values. [Anisole]:[4VP]:[initiator]:[TIPNO] is equal to 499:74:1:0.49.

counterbalancing irreversible termination. Also, the regression lines should theoretically intersect the origin, which is the case for $[4VP]_0$:$[initiator]_0$:$[TIPNO]_0$ equal to 294:1:0.19. This indicates the positive effect of the initial addition of TIPNO. Indeed, with increasing amount of TIPNO, the equilibrium is shifted toward the dormant species (see Scheme 1a), thus avoiding an accumulation of radicals. Therefore, bimolecular termination reactions are limited in the first stage of the polymerization. This analysis is confirmed by the comparison of PDIs. For both experiments, low PDIs were obtained (Figure 3), and the initial PDI values for low conversions depend on the amount of free nitroxide. For the lower amount of TIPNO, the broadening of the molecular weights is higher, giving a PDI of 1.28 at 13.7% conversion (Figure 3a). For comparison, for the polymerization with the higher amount of TIPNO, the PDI is 1.16 at 8.6% conversion (Figure 3b).

This fact supports the beneficial effect of the higher concentration of nitroxide on the initial stage of the process. For both experiments, the molecular weights grow linearly with conversion and fit with the theoretical values of M_n. It should be noted

Scheme 2. Possible Pathways toward Diblock Copolymer Synthesis Starting from P4VP (Method A) or PVDMTPD (Method B) Macroinitiator

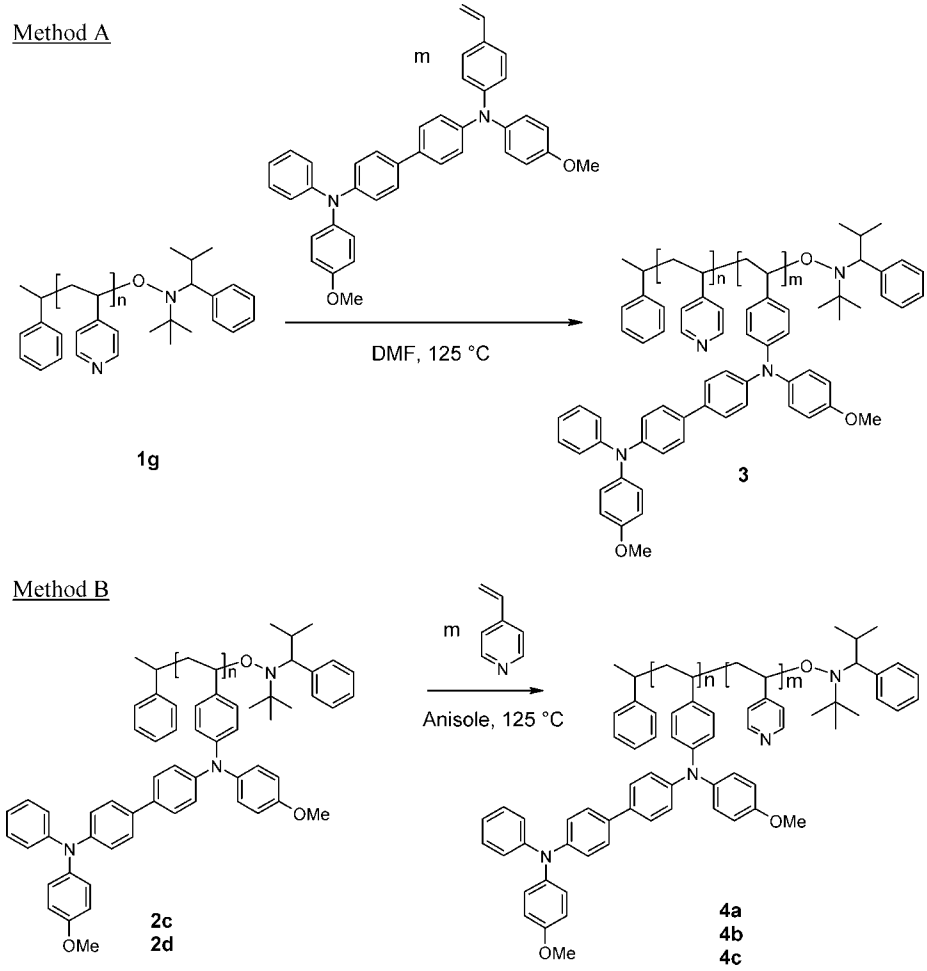

that the molecular weights were measured by SEC calibrated with polystyrene standards, so they may deviate from the real values. Data concerning P4VP samples obtained at different conversions, **1c**−**f**, are shown in Table 1.

NMRP of VDMTPD. The NMRP of VDMTPD with a low polydispersity (PDI ∼ 1.15) has been reported earlier by us.[18] However, the kinetics of polymerization had not been studied in detail, and therefore it was investigated here. For this purpose, a $[VDMTPD]_0$:$[initiator]_0$:$[TIPNO]_0$ molar ratio of 74:1:0.49 was used. In order to withdraw aliquots properly, the viscosity of reaction medium had to be lowered. Therefore, the reaction mixture was diluted by four times with anisole compared to the optimum polymerization conditions reported earlier. Figure 4a shows the plot of $\ln([M]_0/[M])$ vs time. The curved shape of the plot indicates that the concentration of radicals is not constant over the course of the polymerization. Concerning the control of polymerization (Figure 4b), the PDI is quite narrow (<1.3), but the experimental molecular weights M_n are much lower than the expected values and reach a plateau at high conversion. Apparently, side reactions affect the kinetics of the polymerization. Since the conversion increased and the values of M_n remained almost unchanged, permanent termination of the chains and creation of new growing radicals must have occurred. The data of the two samples that were drawn during this polymerization at two different conversions, **2a** and **2b**, are given in Table 1.

This lack of control of polymerization can be rationalized by assuming H transfer from a growing radical chain end to the mediating nitroxide radical, leading to the corresponding hydroxylamine and a dead unsaturated polymer chain end.[26] The hydroxylamine then can be involved in a second H transfer to an active radical, regenerating the nitroxide and giving a second dead chain (saturated). At the same time, new radicals can be created by autoinitiation of the monomer. These side reactions compete with the mechanism of NMRP and become preponderant probably because of the high dilution with anisole.

Synthesis of P4VP-*block*-PVDMTPD (3). Two strategies toward the targeted block copolymer can now be envisaged. The block copolymerization can be started either by using a P4VP (method A) or a PVDMTPD (method B) macroinitiator, which is shown in Scheme 2.

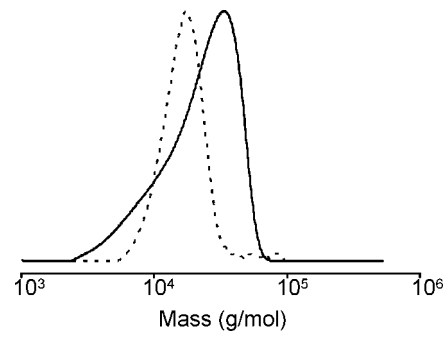

Figure 5. SEC chromatograms of the P4VP macroinitiator **1g** (dots) and the corresponding P4VP-*block*-PVDMTPD polymer **3** (line). 2-*N*-Methylpyrrolidone containing 0.05 M LiBr was used as eluent.

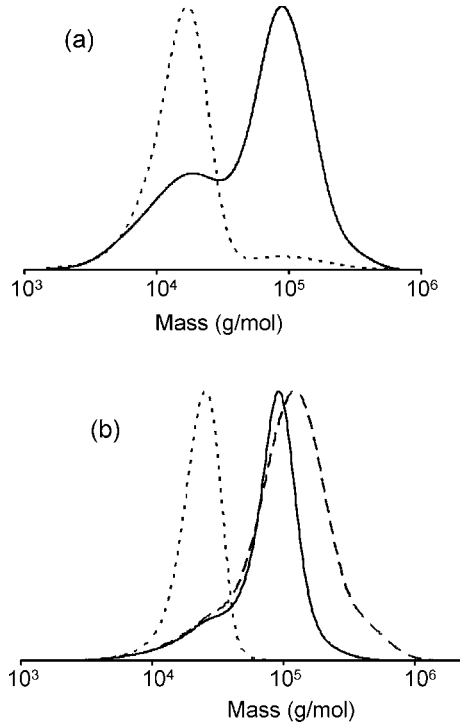

Figure 6. SEC chromatograms: (a) macroinitiator PVDMTPD **2c** (dots) and the corresponding block copolymer P4VP-*block*-PVDMTPD **4a** (lines); (b) macroinitiator PVDMTPD **2d** (dots) and the corresponding block copolymers P4VP-*block*-PVDMTPD **4b** (lines) and **4c** (dashes) obtained at different conversions. 2-*N*-Methylpyrrolidone containing 0.05 M LiBr was used as eluent.

The approach using P4VP as macroinitiator was carried out first (method A in Scheme 2). A crucial problem here to solve is the selection of the correct amount of a suitable solvent. Indeed, the solvent needs to dissolve both the polar P4VP macroinitiator and the monomer VDMTPD, both of which are solids. Dimethylformamide (DMF) was chosen as solvent for the block copolymerization. P4VP macroinitiator **1g** (M_n = 14.8 kg/mol, PDI = 1.15) was used (see Table 1), and the block copolymer synthesis was carried out at a $[VDMTPD]_0$:$[P4VP]_0$:$[TIPNO]_0$ molar ratio of 195:1:0.2. It is important to note that VDMTPD and P4VP were diluted drastically with DMF with $[VDMTPD]_0$ and $[P4VP]_0$ equal to 0.196 and 0.001 mol/L, respectively. This dilution was necessary due to the limited solubility of the components. For comparison, the homopolymerization of VDMTPD was carried out at a concentration of $[VDMTPD]_0$ equal to 3.25 mol/L and $[initiator]_0$ equal to 0.0434 mol/L. The reaction was stopped after 220 min, and the block copolymer **3** was analyzed by SEC (see Figure 5). As can be seen in the chromatogram, the peak shifted only slightly toward higher molecular weights, meaning that the polymerization occurred very slowly. Furthermore, the broadening of SEC trace for the block copolymer toward smaller molecular weights indicates that another polymerization process occurred. Most probably, autoinitiation of VDMTPD took place which would have led to homopolymer PVDMTPD.

Synthesis of PVDMTPD-*block*-P4VP (4a, 4b, 4c). Method B starting from PVDMTPD macroinitiators was tested here with the goal of avoiding homopolymerization of VDMTPD and obtaining well-defined and pure block copolymers, PVDMTPD-*block*-P4VP (Scheme 2).

A first attempt was carried out starting from PVDMTPD macroinitiator **2c** (M_n = 13.3 kg/mol; PDI = 1.23). The molar ratio $[4VP]_0$:$[PVDMTPD]_0$:$[TIPNO]_0$ was equal to 1612:1:0.62, and anisole was also added to facilitate the dissolution of the macroinitiator ([4VP]:[anisole] equal to 5:2 v/v). The results are shown in Figure 6a. The SEC curve of block copolymer **4a** is bimodal, and the superposition with the chromatogram of the macroinitiator clearly shows that initiation was incomplete, leading to a mixture of PVDMTPD and PVDMTPD-*block*-P4VP. Nevertheless, the majority peak is clearly shifted to higher molecular weights relative to the macroinitiator, which demonstrates that a block copolymer with appreciably high molecular weight was generated. The presence of a significant amount of PVDMTPD could be attributed to the low solubility of this polymer in the reaction mixture as well as a significant percentage of dead chains of PVDMTPD in macroinitiator.

In order to avoid this problem, a PVDMTPD macroinitiator **2d** (M_n = 20.8 kg/mol; PDI = 1.15) was synthesized using styrene as comonomer. This should enhance the solubility and also might decrease the amount of dead chain ends of the macroinitiator formed during macroinitiator synthesis. Moreover, the use of styrene as comonomer was also reported to result in a higher degree of control for the NMRP of acrylates[27] and methacrylates.[28] Therefore, we assumed that termination reactions in the polymerization of VDMTPD, as discussed before, might be reduced which finally should lead to a higher initiation efficiency of the block copolymerization. The slight dilution of the DMTPD moieties with an electronically inactive monomer is not expected to lead to a decrease in the charge carrier mobility. This is supported by reports from Borsenberger et al., who found that the charge carrier mobility of hole transport molecules blended in polystyrene was almost maintained for polystyrene weight fractions of up to 60%.[29] A detailed study of the dilution effect of styrene as comonomer on the charge carrier mobility in PVDMTPD is currently underway. The new macroinitiator **2d**, containing a weight fraction of styrene units of 19.3%, was then used for the synthesis of the second block together with a larger amount of anisole ([4VP]:[anisole] equal to 2:1 v/v) and a $[4VP]_0$:$[PVDMTPD]_0$:$[TIPNO]_0$ molar ratio of 2675:1:2.13. Two aliquots were isolated after 1 h (16.5% conversion) and 2 h of reaction time (25.5% conversion), giving block copolymers **4b** and **4c** with 65 and 74 wt % of P4VP, respectively. The molecular weights from SEC chromatograms of **2d**, **4b**, and **4c** are presented in Figure 6b. Clearly, the initiation was more efficient as indicated by the low amount of residual macroinitiator in the block copolymers. Consequently, block copolymers **4b** and **4c** exhibit lower polydispersities than **4a**. The block copolymers **4b** and **4c** are amorphous in nature as determined from differential scanning calorimetry (DSC) measurements and exhibit glass transition temperatures T_g of 155 and 156 °C, respectively. This is in close agreement with the values of the macroinitiators P4VP and PVDMTPD, which show T_g values of 154 and 157 °C, respectively. All data regarding the block copolymers are given in Table 2.

Self-Assembly of PVDMTPD-*block*-P4VP. The morphologies of the newly synthesized block copolymers **4b** and **4c**

Table 2. Polymerization Conditions, Molecular Weights, Polydispersity Indices, and Composition of Block Copolymers 3, 4a, 4b, and 4c (MI, M, and I Correspond to Macroinitiator, Monomer, and Initiator, Respectively)

block copolymer	number	MI	$[M]_0$ (wt %) (solvent)	$[M]_0$:$[I]_0$:$[TIPNO]_0$ molar ratio	M_n (kg/mol)	M_w (kg/mol)	PDI	wt % 4VP
P4VP-*block*-PVDMTPD	**3**	**1g**	10.5 (DMF)	195:1:0.2	15.9	25.4	1.60	
PVDMTPD-*block*-P4VP	**4a**	**2c**	67.5 (anisole)	1612:1:0.62	28.9	81.6	2.82	bim
	4b	**2d**	63.4 (anisole)	2269:1:2.19	52.4	86.5	1.65	65.3
	4c	**2d**	63.4 (anisole)	2269:1:2.19	82.4	146.7	1.78	74.2

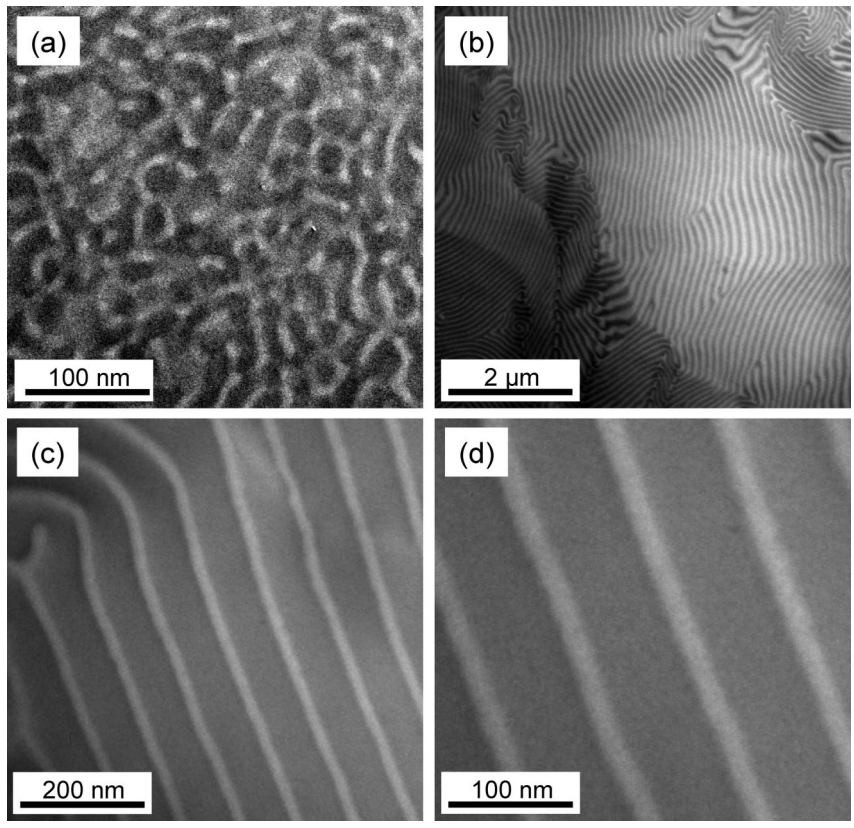

Figure 7. TEM cross sections of block copolymers: (a) bulk sample obtained after thermal annealing of **4b** at 180 °C; (b−d) bulk sample at different magnifications obtained after slowly evaporating a solution of **4c** in pyridine and subsequent annealing at 170 °C for 2 days. All samples were embedded in epoxy resin, cut, and stained with I_2. P4VP and PVDMTPD domains are dark and bright, respectively.

containing a hole conducting block and a 4VP block were then investigated using transmission electron microscopy (TEM). Cross sections of bulk samples can be seen in Figure 7. After staining with iodine, P4VP regions appear dark. The block copolymer **4b** was annealed at 180 °C. The morphology of this diblock copolymer shows disordered short cylinders or wormlike structures of PVDMTPD in a P4VP matrix (Figure 7a). A bulk sample of **4c** was also prepared, but with a different method. Here, a solution of the diblock polymer in pyridine was slowly evaporated at 65 °C and then annealed at 170 °C for 2 days. TEM images of cross sections of resulting thick volume samples with different magnifications displaying a lamellar morphology are shown in Figure 7b−d. The observed lamellae are disordered on the large scale (Figure 7b), but we can observe small-scale alignments of the structure (Figure 7c,d), which probably is due to slow evaporation of pyridine. It is interesting to note that we observed a lamellar structure in our block copolymer (with 74 wt % P4VP), which should rather result in a cylindrical microstructure. Moreover, the lamellae are asymmetric with domain sizes of 20 and 60 nm for PVDMTPD and P4VP, respectively. These two phenomena can be reasonably explained by a high polydispersity of the P4VP block compared to the PVDMTPD block. This is in accordance with reports in literature, where the spacing of one domain was found to enlarge when the PDI of respective block was increased compared to the other block.[30,31] Here even for high percentages of one block, asymmetric lamellae were observed.[32]

Self-Assembly of Hybrid Bulk Samples Containing CdSe:Te Nanocrystals. The newly synthesized block copolymer **4c** was then mixed with CdSe:Te nanocrystals,[33] and the self-assembly behavior was investigated using TEM. CdSe nanoparticles were previously reported to selectively distribute in the P4VP block of polystyrene-*block*-P4VP.[7] The above-mentioned procedure for TEM sample preparation was applied with a solution of **4c** and CdSe:Te nanocrystals (containing 2 mol % of Te and with an average diameter of 3.4 nm) in pyridine. The CdSe:Te nanoparticles were initially stabilized with a three-component mixture of trioctylphosphine, hexadecylamine, and trioctyphosphine oxide, which was partially exchanged with pyridine, in order to provide better affinity for the P4VP domains. TEM images of the bulk nanocomposite samples are presented in Figure 8. No difference in morphology can be observed between the sample simply obtained by slow evaporation in pyridine (Figure 8a,b) and the sample with additional thermal annealing (Figure 8c,d).

Interestingly, the morphology did not change after incorporation of nanocrystals, and the domain sizes for PVDMTPD and P4VP are still around 20 and 60 nm, respectively. The most interesting result concerns the CdSe:Te nanoparticles which are exclusively sequestered in the P4VP domains and preferentially located close to the interface of the two domains. Thus, a fully functionalized nanostructured hybrid nanocomposite material comprised of hole transporting PVDMTPD domains and P4VP domains with sequestered light harvesting/electron conducting CdSe:Te nanocrystals was prepared. These results offer many opportunities to utilize these materials in thin films for future applications in novel device concepts.[34] Since the bulk is completely microphase separated, thicker films of this material for photovoltaic devices can be used, which is of essential advantage in harvesting all the incident light. Still, for this purpose, the concentration of the nanocrystals in P4VP domains has to be increased in order to get efficient light harvesting and charge percolation via nanocrystals, which is the subject matter of our current research.

Conclusion. The polymerizations of 4-vinylpyridine (4VP) and vinyl-*N,N′*-bis(4-methoxyphenyl)-*N,N′*-diphenyl-(1,1′-bi-

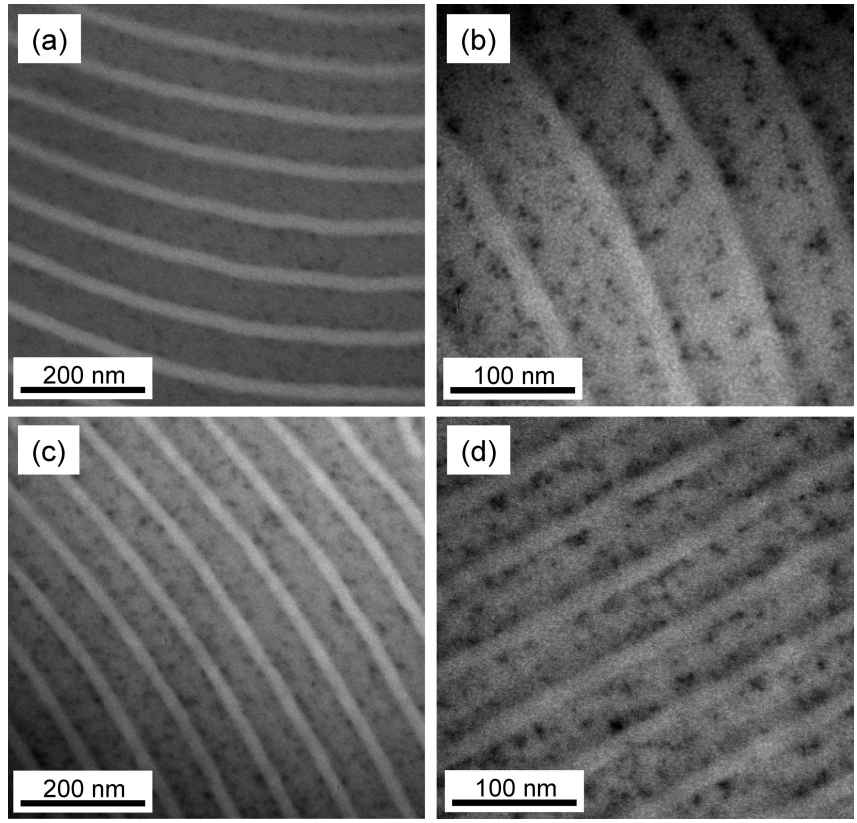

Figure 8. TEM cross sections of composites of block copolymer **4c** and CdSe:Te nanocrystals. All volume samples were obtained after slow evaporation of a solution of CdSe:Te nanoparticles (volume fraction 0.5% to the P4VP block) and **4c** in pyridine. (a) and (b) were not annealed. (c) and (d) were annealed 2 days at 170 °C. The samples were embedded in epoxy resin, cut, and stained with I_2. PVDMTPD domains are bright, and P4VP domains appear darker. The black dots represent the nanocrystals.

phenyl)-4,4′-diamine VDMTPD by nitroxide-mediated radical polymerization were studied and optimized. Moreover, a strategy of block copolymer synthesis of PVDMTPD-*block*-P4VP was developed, and the resulting microphase-separated bulk morphologies were investigated using transmission electron microscopy (TEM). Furthermore, nanocomposites from these functional diblock copolymers and CdSe:Te nanoparticles were successfully prepared and characterized by TEM. This new hybrid semiconductor material exhibits lamellar nanostructures in which the hole conductor domains of PVDMTPD are separated from light harvesting nanocrystals, which are exclusively confined in the P4VP domains. We also find the nanoparticles preferentially located at the domain interface of the lamellar structure. These results show that the challenging task of applying the block copolymer strategy to semiconductor nanocomposites with morphological stability can be realized, making innovative hybrid devices feasible. Potentially, these nanostructures can be varied by changing the length of both blocks or by using different nanoparticles. Thus, future applications such as new photovoltaic or spintronic devices can be envisioned using this exciting material.

Experimental Section

General Information. All glass apparatuses were dried at 115 °C and cooled down under nitrogen. Solvents used for column chromatography and precipitation were distilled before use. TIPNO,[35] alkoxyamine initiator,[31] and VDMTPD[36] were synthesized according to the literature. The synthesis of CdSe:Te nanocrystals was published elsewhere.[33] These nanocrystals was prepared via high-temperature pyrolysis of Cd, Se, and Te precursors (dimethylcadmium, trioctylphosphine selenide, and trioctylphosphine telluride), in a three-component mixture of highly boiling coordinating solvents trioctylphosphine, hexadecylamine, and tri-*n*-octylphosphine oxide. 4-Vinylpyridine (Aldrich, 95%) was dried over calcium hydride, distilled under reduced pressure, and degassed with nitrogen. Anisole and toluene were dried over sodium and distilled under nitrogen. Acetone (VWR, >99.8%) was distilled over anhydrous calcium sulfate and degassed with nitrogen. Dry THF was distilled over Na/benzophenone. DMF was obtained from Fluka and distilled over CaH_2. Diethyl ether was obtained from Riedel-de Haën and used as received. Chloroform was distilled as usual.

Instrumentation. ^{1}H NMR spectra were recorded on a Bruker AC 250 spectrometer (250 MHz). SEC measurements of PVDMTPD were carried out in THF using UV and RI detectors (Waters). For calibration, polystyrene standards and 1,2-dichlorobenzene as an internal standard were used. All the other samples were analyzed using two PSS GRAM 7 μm, 1000 and 100 Å columns at 70 °C with a Waters 486 UV detector and a Bischoff RI-detector 8110. 50 μL of the sample diluted in 2-*N*-methylpyrrolidone containing 0.05 M LiBr was injected. PS standards were used for calibration, and methyl benzoate was used as an internal standard.

Differential scanning calorimetry was carried out at heating rates of 10 K/min between 30 and 200 °C under N_2 with a Perkin-Elmer Diamond DSC.

For TEM sample preparation, molten samples were embedded into epoxy resin, cut, and stained with iodine. Measurements were performed on a Zeiss 902 instrument at 80 kV.

Polymerization Procedures. *Synthesis of P4VP.* A typical procedure is described here as a representative example. A solution of 52 mg (0.159 mmol) of initiator and 7.1 mg (0.032 mmol) of nitroxide in a small amount of chloroform was added to a 10 mL Schlenk tube equipped with a stir bar. Chloroform was evaporated under vacuum. Anisole (1 mL, 9.201 mmol) and 4-vinylpyridine (5 mL, 46.985 mmol) were added to the Schlenk tube under nitrogen, evacuated under vacuum in a liquid nitrogen bath, and backfilled with nitrogen gas. The Schlenk tube was immersed in

an oil bath kept at 125 °C for 76 min. Dilution with chloroform and precipitation (2×) in diethyl ether yielded **1g** as a white powder.

For monitoring kinetics, aliquots were withdrawn periodically from the polymerization medium. Analysis by ^{1}H NMR in $CDCl_3$ was used to determine the conversion (GC and NMR data for monomer consumption were identical).

Synthesis of PVDMTPD.[17] 0.745 g (1.3 mmol) of VDMTPD was taken in a 10 mL flask under nitrogen. A solution of initiator (5.65 mg, 0.0174 mmol) and TIPNO (1.90 mg, 0.0086 mmol) in 400 μL anisole was added. After degassing, the mixture was stirred at 125 °C for 300 min. The polymerization was quenched by rapid cooling. Dilution in toluene and precipitation (2×) in acetone yielded PVDMTPD as a white powder. ^{1}H NMR (250 MHz, CD_2Cl_2): δ (ppm) = 7.10 (br, CHar), 6.88 (br, CHar), 6.80 (br, CHar), 6.53 (br, CHar), 3.76 (br, OCH_3), 3.64 (br, OCH_3), 1.97 (br, CH), 1.57 (br, CH_2).

Synthesis of P4VP-block-PVDMTPD. 0.04 mg (0.181×10^{-3} mmol) of nitroxide in a small amount chloroform was added to a 10 mL Schlenk tube equipped with a stir bar. Chloroform was evaporated under vacuum. 13.4 mg (0.905×10^{-3} mmol) of macroinitiator **1g**, VDMTPD (101.3 mg, 0.177 mmol), and DMF (0.9 mL, 11.624 mmol) were added to the Schlenk tube under nitrogen. The Schlenk tube was evacuated under vacuum in a liquid nitrogen bath, backfilled with nitrogen, and immersed in an oil bath heated to 125 °C. The polymerization was stopped by rapid cooling. Dilution in chloroform and precipitation in diethyl ether yielded P4VP-*block*-PVDMTPD as a white solid.

Synthesis of PVDMTPD-block-P4VP. 3.3 mg (0.015 mmol) of nitroxide in a small amount chloroform was added to a 10 mL Schlenk tube equipped with a stir bar. Chloroform was evaporated under vacuum. 144 mg (7.03×10^{-3} mmol) of PVDMTPD, 1 mL of anisole (1 mL, 9.201 mmol), and 4-vinylpyridine (2 mL, 18.794 mmol) were added under nitrogen. The Schlenk tube was evacuated under vacuum in a liquid nitrogen bath, backfilled with nitrogen, and immersed in an oil bath heated to 125 °C. The polymerization was stopped by rapid cooling after 120 min. Dilution in chloroform and precipitation in diethyl ether (3×) yielded PVDMTPD-*block*-P4VP as a white solid. ^{1}H NMR (250 MHz, CD_2Cl_2): δ (ppm) = 8.30 (br, CHar 4VP), 7.15 (br, CHar TPD), 6.98 (br, CHar VDMTPD), 6.78 (br, CHar VDMTPD), 6.43 (br, CHar 4VP), 3.66 (br, OCH_3), 3.44 (br, OCH_3), 1.81 (br, CH, 4VP), 1.51 (br, CH_2, 4VP).

Acknowledgment. The Bayreuth group acknowledges the financial support from DFG as part of European Science Foundation EUROCORES programme under SONS II, SOHYDs, and SFB 481 for this research work. A.L.R. and D.V.T. are grateful to the German Excellence Initiative for funding via the "Nanosystems Initiative Munich (NIM)" and the LMUexcellent program. We also thank Carmen Kunert and Sabine Wunder for the TEM and the SEC measurements, respectively.

References and Notes

(1) Beecrof, L. L.; Ober, C. *Chem. Mater.* **1997**, *9*, 1302–1317.
(2) Haryono, A.; Binder, W. H. *Small* **2006**, *5*, 600–611.
(3) Beek, W. J. E.; Wienk, M. M.; Janssen, R. A. J. *Adv. Mater.* **2004**, *16*, 1009–1013.
(4) Liang, L.; Dzienis, K. L.; Wang, Q. *Adv. Funct. Mater.* **2006**, *16*, 542–548.
(5) Gur, I.; Fromer, N. A.; Chen, C.-P.; Kanaras, A. G.; Alivisatos, A. P. *Nano Lett.* **2007**, *7*, 409–414.
(6) Yeh, S.-W.; Wei, H.-H.; Sun, Y.-S.; Jeng, U-S.; Liang, K. S. *Macromolecules* **2005**, *38*, 6559–6565.
(7) Lin, Y.; Böker, A.; He, J.; Sill, K.; Xiang, H.; Abetz, C.; Li, X.; Wang, J.; Balazs, A.; Russell, T. P. *Nature (London)* **2005**, *434*, 55–59.
(8) Lo, C.-T.; Lee, B.; Winans, R. E.; Thiyagarajan, P. *Macromolecules* **2006**, *39*, 6318–6320.
(9) Chiu, J. J.; Kim, B. J.; Yi, G.-R.; Bang, J.; Kramer, E. J.; Pine, D. J. *Macromolecules* **2007**, *40*, 3361–3365.
(10) Bockstaller, M. R.; Mickiewicz, R. A.; Thomas, E. L. *Adv. Mater.* **2005**, *17*, 1331–1349.
(11) Förster, S.; Antonietti, M. *Adv. Mater.* **1998**, *10*, 195–217.
(12) Balazs, A. C.; Emrick, T.; Russell, T. P. *Science* **2006**, *314*, 1107–1110.
(13) Mackay, M. E.; Tuteja, A.; Duxbury, P. M.; Hawker, C. J.; Van Horn, B; Guan, Z.; Chen, G.; Krishnan, R. S. *Science* **2006**, *311*, 1740–1743.
(14) Li, C.-P.; Wei, K.-H.; Huang, J. Y. *Angew. Chem., Int. Ed.* **2006**, *45*, 1449–1453.
(15) Krishnan, K. M.; Pakhomov, A. B.; Bao, Y.; Blomqvist, P.; Chun, Y; Gonzales, M.; Griffin, X.; Ji, X.; Roberts, B. K. *J. Mater. Sci.* **2006**, *41*, 793–815.
(16) Lindner, S. M.; Thelakkat, M. *Macromolecules* **2004**, *37*, 8832–8835.
(17) Lindner, S. M.; Hüttner, S.; Chiche, A.; Thelakkat, M.; Krausch, G. *Angew. Chem., Int. Ed.* **2006**, *45*, 3364–3368.
(18) Sommer, M.; Lindner, S. M.; Thelakkat, M. *Adv. Funct. Mater.* **2007**, *17*, 1493–1500.
(19) Creutz, S.; Teyssier, P.; Jérôme, R. *Macromolecules* **1997**, *30*, 1–5.
(20) Xia, J.; Zhang, X.; Matyjaszewski, K. *Macromolecules* **1999**, *32*, 3531–3533.
(21) Convertine, A. J.; Sumerlin, B. S.; Thomas, D. B.; Lowe, A. B.; McCormick, C. L. *Macromolecules* **2003**, *36*, 4679–4681.
(22) Fischer, A.; Brembilla, A.; Lochon, P. *Macromolecules* **1999**, *32*, 6069–6072.
(23) Diaz, T.; Fischer, A.; Jonquières, A.; Brembilla, A.; Lochon, P. *Macromolecules* **2003**, *36*, 2235–2241.
(24) Bohrisch, J.; Wendler, U.; Jaeger, W. *Macromol. Rapid Commun.* **1997**, *18*, 975–982.
(25) Lohmeijer, B. G. G.; Schubert, U. S. *J. Polym. Sci., Part A* **2005**, *43*, 6331–6344.
(26) Hawker, C. J.; Bosman, A. W.; Harth, E. *Chem. Rev* **2001**, *101*, 3661–3688.
(27) Fukuda, T.; Terauchi, T.; Goto, A.; Tsujii, Y.; Miyamoto, T. *Macromolecules* **1996**, *29*, 3050–3052.
(28) Charleux, B.; Nicolas, J.; Guerret, O. *Macromolecules* **2005**, *38*, 5485–5492.
(29) Borsenberger, P. M.; Gruenbaum, W. T.; Wolf, U.; Bässler, H. *Chem. Phys.* **1998**, *234*, 277–284.
(30) Lynd, N. T.; Hamilton, B. D.; Hillmyer, M. A. *J. Polym. Sci., Part B* **2007**, *45*, 3386–3393.
(31) Lynd, N. T.; Hillmyer, M. A. *Macromolecules* **2005**, *38*, 8803–8810.
(32) Ruzette, A.-V.; Tencé-Girault, S.; Leibler, L.; Chauvin, F.; Bertin, D.; Guerret, O.; Gérard, P. *Macromolecules* **2006**, *39*, 5804–5814.
(33) Franzl, T.; Müller, J.; Klar, T. A.; Rogach, A. L.; Feldmann, J.; Talapin, D. V.; Weller, H. *J. Phys. Chem. C* **2007**, *111*, 2974–2979.
(34) Holder, E.; Tessler, N.; Rogach, A. L. *J. Mater. Chem.* **2008**, *18*, 1064–1078.
(35) Benoit, D.; Chaplinski, V.; Braslau, R.; Hawker, C. J. *J. Am. Chem. Soc.* **1999**, *121*, 3904–3920.
(36) Schmitz, C.; Thelakkat, M.; Schmidt, H. W. *Adv. Mater.* **1999**, *11*, 821–826.

MA8007459